International Journal of Thermal Technologies
E-ISSN 2277 – 4114

Available at http://inpressco.com/category/ijtt/

Research Article

A Study on Pressure Distribution in Miniature Neutron Source Reactor (MNSR) Core Coolant

Salihu Mohammed* **and Musa B. Likita**

Department of Physical Sciences, Niger State Polytechnic, Zungeru. Niger State, Nigeria

Accepted 25 May 2016, Available online 30 June 2016, **Vol.6, No.2 (June 2016)**

Abstract

Measuring systems for monitoring of flow parameters whose magnitude and limits accounts for the integrity of the core is an important safety consideration in nuclear reactor design. The present work employs STAR-CCM+ CFD code–based Reynold's Averaged Nervier Stokes equations (RANS) to solve transported variables -Turbulence kinetic energy and its dissipation rate to study pressure distribution in the core coolant of Miniature Neutron Source Reactor (MNSR). A cylindrical symmetry of the reactor core was modeled to equal a tenth of MNSR's nuclear fuel element to represent the coolant. This was further segmented into 21 equal axial lengths. To conform with the non-uniform heat fluxes imposed on reactor core coolant by the fuel pins at nominal operation, heat fluxes computed using Monte Carlo Neutron Particle (MCNP) code were imposed on the wall surfaces of corresponding segments. The initial conditions common to Ghana Research Reactor-1 (GHARR-1) and Nigerian Research Reactor-1 (NIRR-1) operational specifications were imposed at the inlet and outlet of the core coolant to initialize the simulation. Results from the simulation were validated with experimental data generated using GHARR-1 and verified with literature on NIRR-1. The result obtained attests to the effectiveness of the primary coolant in safely removing the generated heat produced in the core of MNSR-type reactor fuel elements.

Keywords: *Research Reactors; STAR-CCM+; RANS; Fuel element; NIRR-1, GHARR-1*

1. Background

The MNSR is a low power reactor with a maximum thermal power output of 31 kW. It utilizes 90% enriched U-235 with 344 fuel pins (in case of GHARR-1) to 347 fuel pins (in case of NIRR-1) capable of generating a thermal flux of up to $1x10^{12}$ $cm^{-2}s^{-1}$. In general, the purpose of MNSR is not for energy generation but for neutron generation for experimental purposes, reactor physics education and training. Countries currently using MNSR include China, Ghana, Iran, Nigeria, Pakistan and Syria. Figure 1 depicts the core arrangement for MNSRs.

Majority of research reactors are characterized by similar design parameters (H. Christos, 2000). Specifications drawn from GHARR-1/NIRR-1 reactors as presented in (M. Salihu, 2016; S. A. Jonah and Y. V. Ibrahim, 2012) were adopted for the present experimentation and simulation references. The use of simulation for thermal hydraulic behavior have been previously reported (H. Tewfik *et al,* 2008). Table 1 and Table 2 provides the technical and physical specifications for MNSR respectively.

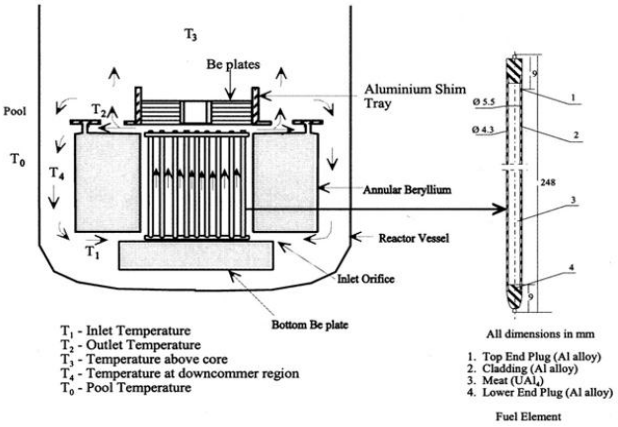

Figure 1: Heat transfer mechanism in MNSR (E. Ampomah-Amoako *et al,* 2009).

Table 1: Reference Design Specifications

S/No	Geometries	Dimensions
1	Core Shape	Cylinder
2	Core height	23 cm
5	Fuel rod diameter (external)	5.5 mm
6	Fuel rod diameter (external)	4.3 mm
12	Number of control rods	1
16	Number of Segmentation	21
17	Segment Length	10.95 mm

*Corresponding author: **Salihu Mohammed**

Table 2: Physics Specification

S/No	Initial Conditions	Magnitude
1	Pressure at inlet	1 bar
2	Flow rate	400L/h (0.111 kg/s)
3	Density of water	999.7 kg/ m3
4	Initial temperature used	307.15 K
5	Power	15 KW
6	Velocity	0.002 m/s

In the case of reactors that utilizes forced circulation to remove the core heat, the primary coolant flow measurement is usually a safety parameter, since it gives a fast indication of degradation of the capability to remove the energy produced in the reactor (F. Brollo *et al,* 2014). The present work performs safety evaluations using Simulation of Turbulent flow in Arbitrary Regions Computational Continuum Mechanics C++ based (STAR-CCM+) CFD code to provide simulations on pressure trend as a function of mass flow rate in the modelled flow domain. Setting up the simulation for the pressure drop was done by specifying the initialization inlet pressure of 1 bar and allowing the system to adjust the inputted pressure to what is most suitable at both the inlet and outlet.

2. Simulation model and computation

2.1 STAR-CCM+ CFD code

STAR-CCM+ is a computational fluid dynamics (CFD) code is structured around numerical algorithms that can tackle fluid flow problems accounting for turbulence effects (H. K. Versteeg and W. malalasekera, 2007) as it employs the Finite Volume Approach to address a wide variety of modeling needs. CFD codes comprise of pre-processor, solver and post-processor phases. The preprocessing is concerned with the geometry modelling, definition of material properties, mesh generation and physics definition (S. T. Sunniya, 2013; V. Y. Agbodemegbe *et al*, 2015). The CFD codes solver section deals with the solver type specification and analysis runs. It solves the transport equations on every node defined during the mesh generation step and any additional models specified in the physics set up (V. Ganesh, 2012). For post processing, CFD codes allow for setting different plots and scenes either before, during or after running the simulation. These plots and scenes are then analyzed on attainment of convergence of the solution. Details of the geometry, meshing and physics models used are published in (M. Salihu, 2016)

2.2 Adopted Solver Equations

Mass conservation, momentum, energy and turbulent transport equations applicable for the k-epsilon turbulent model employed for this study are presented in equations (1) to (7) (STAR CCM+ User Guide, 2011).

2.2.1 Continuity Equation

$$\frac{\partial \rho}{\partial t}+\frac{\partial(\rho u)}{\partial x}+\frac{\partial(\rho v)}{\partial y}+\frac{\partial(\rho w)}{\partial z}=0 \quad (1)$$

where ρ is the density, t is time (s), *u, v and w* are components of velocity corresponding to *x, y and z* planes respectively.

2.2.2 Momentum Equations

U- Momentum

$$\frac{\partial(\rho U)}{\partial t}+\frac{\partial}{\partial x}\left(\rho U^2-\mu e\frac{\partial U}{\partial x}\right)+\frac{\partial}{\partial y}\left(\rho UV-\mu e\frac{\partial U}{\partial y}\right)+\frac{\partial}{\partial z}\left(\rho UW-\mu e\frac{\partial U}{\partial z}\right)=-\frac{\partial p}{\partial x}+\rho\ \mathrm{g\_x} \quad (2)$$

V- Momentum

$$\frac{\partial(\rho U)}{\partial t}+\frac{\partial}{\partial x}\left(\rho UV-\mu e\frac{\partial U}{\partial x}\right)+\frac{\partial}{\partial y}\left(\rho V^2-\mu e\frac{\partial U}{\partial y}\right)+\frac{\partial}{\partial z}\left(\rho VW-\mu e\frac{\partial V}{\partial z}\right)=-\frac{\partial p}{\partial y}+\rho g_y \quad (3)$$

W-Momentum

$$\frac{\partial(\rho W)}{\partial t}+\frac{\partial}{\partial x}\left(\rho UW-\mu e\frac{\partial W}{\partial x}\right)+\frac{\partial}{\partial y}\left(\rho VW-\mu e\frac{\partial W}{\partial y}\right)+\frac{\partial}{\partial z}\left(\rho W^2-\mu e\frac{\partial W}{\partial z}\right)=-\frac{\partial p}{\partial z}+\rho g_z \quad (4)$$

where, ρ is the density of the fluid, P is the pressure, and τ is the viscous stress

2.3 Energy Equation

$$\rho\frac{DE}{Dt}=-div(pu)+\left[\frac{\partial(u\tau_{xx})}{\partial x}+\frac{\partial(u\tau_{yx})}{\partial y}+\frac{\partial(u\tau_{zx})}{\partial z}+\frac{\partial(v\tau_{xy})}{\partial x}+\frac{\partial(v\tau_{yy})}{\partial y}+\frac{\partial(v\tau_{zy})}{\partial z}+\frac{\partial(w\tau_{xz})}{\partial x}+\frac{\partial(w\tau_{yz})}{\partial y}+\frac{\partial(w\tau_{zz})}{\partial z}+div(kgradT)+S_E\right] \quad (5)$$

2.4 k-ε turbulence equation

$$\frac{d}{dt}\int_V \rho k dV+\int_A \rho k\left(v-v_g\right).da=\int_A\left(\mu+\frac{\mu_t}{\sigma_k}\right)\nabla k.da+\int_V\left[G_k+G_b-\rho\left((\varepsilon-\varepsilon_o)+\square_m\right)+S_k\right]dV \quad (6)$$

$$\frac{d}{dt}\int_V \rho\varepsilon dV+\int_A \rho\varepsilon\left(v-v_g\right).da=\int_A(\mu+\frac{\mu_t}{\sigma_\varepsilon})\nabla\varepsilon.da+\int_V\frac{1}{T}\left[C_{\varepsilon1}(G_k+G_{nl}+C_{\varepsilon3}G_b)-C_{\varepsilon2}\rho\left((\varepsilon-\varepsilon_o)+\rho\square_y\right)+S_\varepsilon\right]dV \quad (7)$$

where S_k and S_ε are the user-specified source terms. ε_o is the ambience turbulence value in source terms that counteract turbulence decay (E. H. K. Akaho and B. T . Maaku, 2002; R. Appiah, 2011).

The code was executed and the equations were solved and monitored to converge by assessing the residuals and the trend of the outlet temperature. The measure of convergence for the present work is presented in Figure 2.

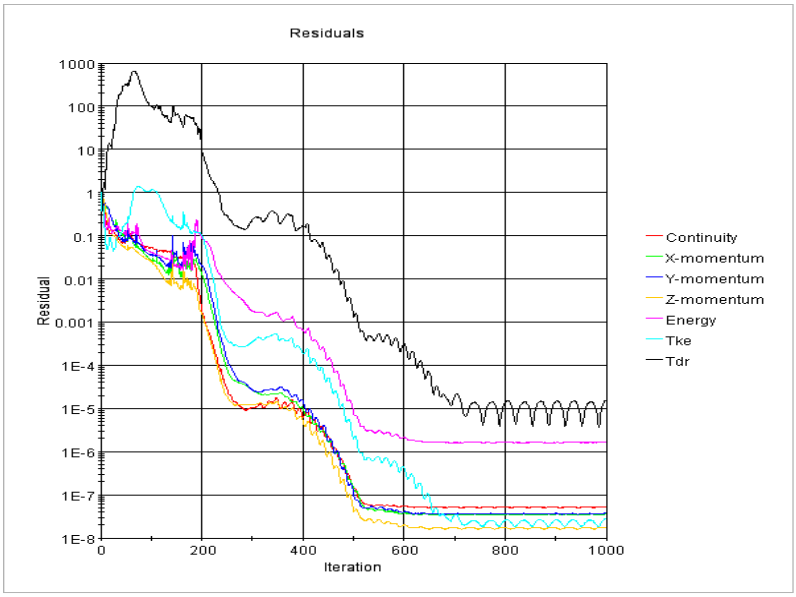

Figure 2: Convergence monitor residual plots

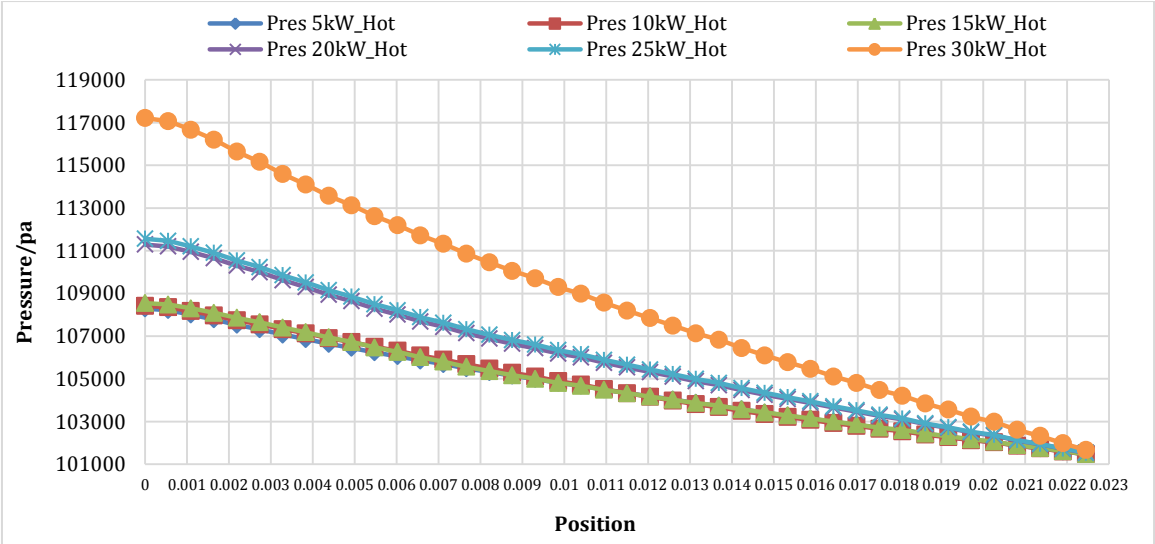

Figure 3: Fluid Centerline Pressure versus Position for hottest channel

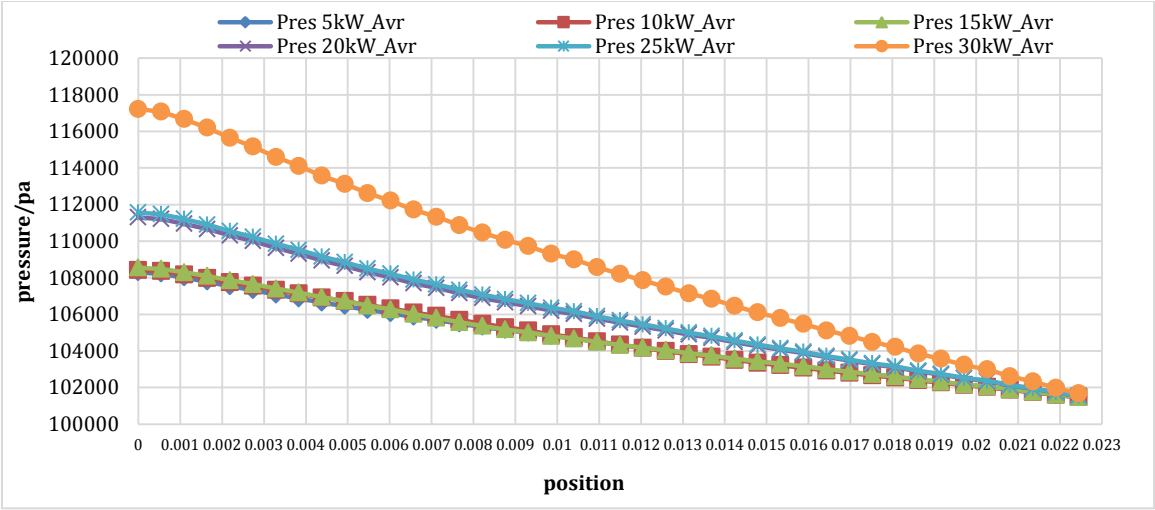

Figure 4: Fluid Centerline Pressure versus Position for averaged channel

3. Result and discussion

The channel centerline pressure was taken using a line probe placed at the center of the geometry. The probe points gives the value of pressure, trends of the pressure across the domain. Figures 3 and 4 show the plot of fluid centerline pressure versus position for simulation at 5 kW to 30 kW for average and hottest channel respectively. "Pres 5kW_Hot and Pres 5kW_Avr" used in the legend are abbreviations for channel centerline pressure taken over each segment for the simulation at 5 kW for the hottest channel and averaged channel respectively.

The pressure at the inlet gives the required pressure for system start-up. The trends show that inlet pressure needed increases with increasing power. The difference between the inlet and outlet pressure for specified power level presented in Figure 3 and 4 and computed using equation 8, gives the required pressure drop needed to push the fluid from inlet to outlet.

$$P_{Di} = P_{Oi} - P_{Ii} \quad (8)$$

where i is the mass flow rate of interest for a specific power, P_D, is the pressure drop, P_O is the outlet pressure and P_I is the inlet pressure . This pressure drop trend conforms to that reported in literature (Y. Yizhou and N. S. Rizwan-Uddin, 2005).

The computed pressure drop for specified mass flow rates imposed on the simulation at 30 kW power for hottest channel is presented in Table 3.

Table 3: Mass flow rate and pressure drop for 30 kW power

Mass flow rate	Outlet pressure	Inlet pressure	Pressure drop
0.15	101493.2	109299.8	7806.6
0.2	101592.6	113884.7	12292.1
0.23	101671.4	117213.3	15541.9

Table 3 shows that an increase in mass flow rate lead to increase in the corresponding pressure drop required to push the fluid out of the system.

Conclusion

A study of pressure distribution as a function of mass flow rate was conducted to evaluate the steady state thermal hydraulic behavior of MNSR core under natural convection cooling. The fluid centerline pressure was found to increase with increase in power, this suggest that both the required pressure for starting the system and the required pressure drop for transporting the fluid across the domain increases with power increase. The range of flow rates obtained from the simulation lies between that quoted SAR (E. H. K Akaho *et al,* 2006) and the value previously reported (M. Salihu, 2016; S. A. Jonah and Y. V. Ibrahim, 2012). The results effectively confirmed the existence of a range of mass flow rates for which core safety is maintained at nominal operation. In addition to setting operational limits, the result presented will improve on the assumption of a stated fixed mass flow rates for MNSR as reported (E. H. K Akaho *et al,* 2006).

Acknowledgements

Developers of STAR-CCM+ (CD-ADAPCO), Niger State Polytechnic Zungeru Nigeria, SNAS University of Ghana, Ghana Atomic Energy Commission, Rijau LGA Community.

References

Agbodemegbe V.Y., Cheng X, Akaho E.H.K, Allotey F.K.A. (2015). Correlation for Cross-Flow Resistance Coefficient Using STAR-CCM+ Simulation Data for Flow of Water through Rod Bundle Supported by Spacer Grid with Split-Type Mixing Vane. *Nuclear Engineering and Design* 285: 134–149.

Ampomah-Amoako E., Akaho E.H.K., Anim-Sampong S., Nyarko B.J.B. (2009). Transient Analysis of Ghana Research Reactor-1 using PARET/ANL thermal–hydraulic code. *Nuclear Engineering and Design* 239: 2479–2483.

Akaho E.H.K., Maaku B.T., Anim Sampong S., Emi-Reynolds G, Boadu H.O, , Dodoo-Amoo D.N.A. (2006). *Ghana Research Reactor-1, Final Safety Analysis Report*. GAEC, Kwabenya, Ghana.

Ampomah-Amoako E. (2013). Stability and control of Supercritical Water Reactor System; A Study into Concepts and Applications. A Nuclear Engineering *Ph.D. Dissertation* Submitted to the University of Ghana.

Akaho E. H., Maaku B. T. (2002). Simulation of transients in a Miniature Neutron Source Reactor core. Nuclear Engineering and Design. 213:1 31-42

Appiah R. (2011). Steady State Thermal-Hydraulics Analysis of GHARR-1 using the PL TEMP/ANL v4.0 Code. University of Ghana, Accra, Ghana.

Brollo F., Cantero P., Almonacid A. (2014). A Core Pressure Drop Monitoring System Design and implementation at the RA6 Research Reactor. *IGORR* Conference.

Christos H. (2000). Simulation of loss-of-flow transients in research reactors. *Annals of Nuclear Energy*, 27, 1683-1693.

Ganesh V. (2012). Understanding CFD Simulation Process with Examples https://ganeshvisavale.wordpress.com/2012/12/07/understanding-cfd-simulation-process-with-examples/.

Jonah S.A., Ibrahim Y.V. (2012). Steady State Thermal Hydraulic Operational Parameters and Safety Margins of NIRR-1 with LEU fuel using PLTEMP-ANL Code. *Transactions Research Reactors ENS Conference.* Manchester, united kingdom. Pp 20-40.

STAR-CCM+ User Guide version 6.04.014 CD_ADAPCO 2011.

Salihu M. (2016). Investigation of Heat Transfer and Distribution in the Core of Ghana Research Reactor-1 (GHARR-1) using STAR-CCM+ CFD Code. An *MPhil. Thesis* Submitted to the University of Ghana.

Sunniva S. T. (2013). Simulation of Viscous Flow around a Circular Cylinder with STAR-CCM+. A *Master's Degree Thesis* submitted to the Norwegian University of Science and Technology, Department of Marine Technology.

Tewfik H., Anis B., El Khider S., Francesco D. (2008). Overview of accident analysis in nuclear research reactors. *Nuclear Energy* 50 7e14.

Versteeg H. K., Malalasekera, W. (2007). *An Introduction to Computational Fluid Dynamics*, the Finite Volume Method. Second edition, pp. 54-128.

Yizhou Y., Rizwan-uddin N. S. (2005). CFD Simulation of a Research Reactor. Mathematics and Computation, Supercomputing, Reactor Physics and Nuclear and Biological Applications, *Palais des Papes,* Avignon, France.